

Effects of quantum mechanics on the deflagration threshold in the molecular magnet Mn_{12} acetate

F. Macià,¹ J. M. Hernandez,¹ J. Tejada,¹ S. Datta,² S. Hill,² C. Lampropoulos,³ and G. Christou³

¹*Departament de Física Fonamental, Facultat de Física, Universitat de Barcelona, Avinguda Diagonal 647, Planta 4, Edifici nou, 08028 Barcelona, Spain*

²*Department of Physics, University of Florida, Gainesville, Florida 32611, USA*

³*Department of Chemistry, University of Florida, Gainesville, Florida 32611, USA*

(Received 22 January 2009; published 12 March 2009)

We report experimental studies of the stability of a Mn_{12} -Ac crystal against magnetic avalanches as a function of the magnitude and direction of the magnetic field, as well as a function of temperature. Strong evidence for quantum effects associated with this phenomenon is seen in the (H_z, H_x) metastability diagram. The data provide further support to the theory of magnetic deflagration.

DOI: [10.1103/PhysRevB.79.092403](https://doi.org/10.1103/PhysRevB.79.092403)

PACS number(s): 75.50.Xx, 45.70.Ht, 76.60.Es, 82.33.Vx

One can ignite fire in a flammable material by slowly raising its temperature.¹ Historically this phenomenon was studied to estimate the danger of a spontaneous combustion due to overheating of a storage containing flammable substances. The rate of a chemical reaction associated with burning is given by $\tau_0^{-1} \exp[-U/(k_B T)]$, where U is the energy barrier, T is the absolute temperature, k_B is the Boltzmann constant, and τ_0 is a prefactor (the so-called attempt time). At a finite temperature $T \ll U$, an exponentially small number of molecules will react and release heat. This heat will flow out of the sample, creating a steady and smooth temperature profile along the substance with a slightly higher temperature in the bulk compared to the temperature at the surface, T_0 , which can be found by equating the heat flow through the boundary to the heat production due to the chemical reaction inside the substance. The temperature profile is entirely determined by T_0 , the shape of the flammable substance, and the thermal conductivity. As T_0 goes up, so does the temperature difference between the surface and the bulk. It turns out that, above a certain value of T_0 , the smooth and steady temperature profile becomes unstable against the formation of a narrow high-temperature burning front (deflagration) that propagates through the substance. Recently it was demonstrated that a very similar phenomenon—magnetic deflagration—is possible in crystals of molecular magnets placed in a magnetic field.^{2,3} In such crystals the role of the chemical energy is played by the Zeeman energy, and the energy barrier, U , for magnetic deflagration can be continuously varied via the external magnetic field. The roles of fuel and ashes (remaining and burned substance) are played by molecules being in either a metastable state (before burning) or stable state (after burning). This allows comprehensive nondestructive studies of deflagration that is not possible with flammable chemical substances.

Molecular magnets attracted considerable attention in the magnetism community after it was shown that individual molecules behave as superparamagnetic particles (see, e.g., Ref. 4). The magnetic bistability⁵ of these molecules is caused by their large spin, $S=10$ for Mn_{12} -Ac, and by strong magnetic anisotropy, D , that provides a large energy barrier between spin-up and spin-down states.

At low temperature, a magnetized crystal of magnetic

molecules exhibits two modes of relaxation. The first, slow mode, is usually observed in magnetic hysteresis by slowly sweeping the magnetic field. It manifests itself in a staircase hysteresis curve⁶ due to quantum tunneling of the magnetic moment between crossing spin states. The second relaxation mode, an avalanche, is a much more rapid magnetization reversal that typically lasts a few milliseconds.⁷⁻⁹ During an avalanche the heat released in the magnetic relaxation further accelerates relaxation. Recent experiments on avalanches in Mn_{12} -Ac have demonstrated that the avalanche is equivalent to deflagration, with the front of the magnetization reversal moving along the sample at 1–10 m/s³. One of the most remarkable features of magnetic deflagration, which does not exist in chemical combustion, is the appearance of quantum maxima in the deflagration speed.² This occurs due to resonant tunneling between quantum spin levels. Additionally, it has been also shown that the required temperature to ignite avalanche at particular values of the longitudinal field, h_z , presents dips at resonant fields.¹⁰

In this Brief Report we study the deflagration threshold in Mn_{12} -Ac in a magnetic field applied at an angle with respect to the anisotropy axis. In a first approximation the magnetic Hamiltonian of the crystal is

$$H = -DS_z^2 - h_z S_z - h_x S_x, \quad (1)$$

where $\mathbf{h} = g\mu_B \mathbf{H}$. To switch from spin-up to spin-down states the system must overcome an energy barrier, U ($=DS^2$ for $\mathbf{h}=0$). The field dependence of U for a metastable population of spins is displayed in Fig. 1 for both the (a) classical and (b) quantum cases. Note that when h_z is opposite to the direction of the magnetization (metastable situation), then both h_z and h_x reduce the energy barrier.

The cross section of the plot in the plane $U=0$ [see white line in Fig. 1(a)] is the classical astroid known from the theory of superparamagnetic particles (see, e.g., Ref. 4).

In addition to a classical reduction in the barrier, h_z can drive the crystal in and out of tunneling resonances, while h_x controls the (nonzero) tunneling rate. In practice, the splitting, $\Delta_{mm'}$, of the (m, m') resonance is small compared to the widths, $\gamma_{m,m'}$, of the tunneling levels due to spin-phonon and other decay processes. In this case, the spin does not coher-

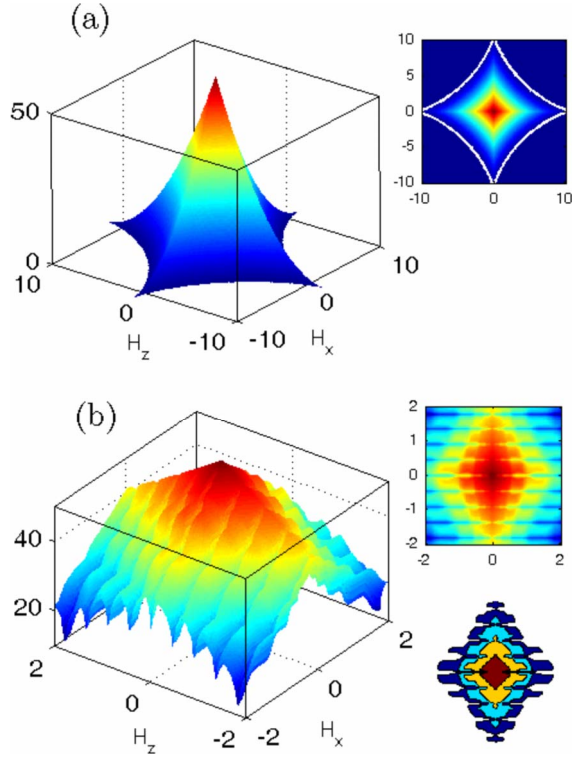


FIG. 1. (Color online) Three-dimensional plot of the energy barrier (in kelvins) as a function of longitudinal and transverse components of the magnetic field (in teslas). Insets show a set of horizontal cross sections of the plot. (a) The energy barrier for a classical spin vector with energy given by Eq. (1); the $T=0$ cross section is the Stoner-Wolfarth astroid. (b) The effective energy barrier for a quantum spin described by the Hamiltonian of Eq. (1); the right lower panel shows cross sections for energies $U=35$, $U=40$, $U=45$, and $U=50$ K.

ently oscillate between m and m' but irreversibly decays to the ground state $m=S$ after incoherently tunneling from m to m' . The corresponding rate of the quantum transition to the stable well from level m is given by^{11,12}

$$\Gamma_m = \frac{\Delta_{mm'}^2}{2\hbar^2} \frac{\gamma_{m'}/2}{\omega_{mm'}^2 + (\gamma_{m'}/2)^2}, \quad (2)$$

where $\hbar\omega_{mm'} = \epsilon_m - \epsilon_{m'}$ is the detuning of the m th and m' th levels. For Hamiltonian (1), the tunnel splitting is given by⁴

$$\Delta_{mm'} = \frac{2D}{[(m' - m - 1)!]^2} \sqrt{\frac{(S+m')!(S-m)!}{(S-m')!(S+m)!}} \left(\frac{h_x}{2D}\right)^{m'-m}. \quad (3)$$

Once Γ_m exceeds the thermally activated relaxation rate from the m th level, the barrier is effectively reduced due to under-barrier tunneling from the m th level. A three-dimensional plot of the effective energy barrier, $U_{\text{eff}}(h_x, h_z)$, which takes account of quantum tunneling and inhomogeneous broadening of the energy levels is shown in Fig. 1(b).

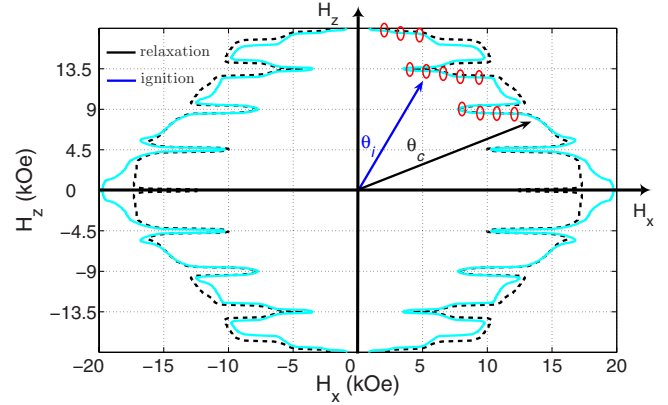


FIG. 2. (Color online) Area of stability against ignition of avalanches (straight cyan curve) and against slow relaxation (dashed black curve). Red circles show points where avalanches should occur when sweeping the field back and forth at a given angle θ_i within the first quadrant. The angle θ_c denotes to the crossing point between the slow relaxation and avalanche stability areas.

According to the theory of magnetic deflagration,¹³ the threshold for ignition of the deflagration front is achieved when the rate, Γ , of the transition out of the metastable well exceeds a critical value,

$$\Gamma_c = \frac{8\kappa(T_0)k_B T_0^2}{U_{\text{eff}}\Delta E n_{-i} l^2}. \quad (4)$$

Here, $\kappa(T_0)$ is the thermal conductivity at $T=T_0$, $U_{\text{eff}}(H)$ and $\Delta E(H)$ are the field-dependent effective energy barrier and the energy difference between spin-up and spin-down ground states, respectively, l is a characteristic length of order the smallest dimension of the sample, and n_{-i} is the initial fraction of molecules available for burning, which can be expressed in terms of the initial (negative) magnetization M_i and the saturation magnetization M_0 as $n_{-i} = (M_0 - M_i)/(2M_0)$. Writing Γ as $\tau_0^{-1} \exp[-U_{\text{eff}}/(k_B T)]$, one obtains the condition for ignition

$$U_{\text{eff}}(h_x, h_z) \Delta E \exp\left[-\frac{U_{\text{eff}}}{k_B T_0}\right] = \frac{8\tau_0 \kappa(T_0) k_B T_0^2}{n_{-i} l^2}. \quad (5)$$

If the field is small compared to the anisotropy field (~ 10 T for $\text{Mn}_{12}\text{-Ac}$), the parameters on the right-hand side of this equation must have only weak dependence on the field, while U_{eff} and ΔE on the left-hand side depend strongly on the field. Consequently, the stability diagram $h_z(h_x)$ can be approximated by the equation $U_{\text{eff}}(\mathbf{h})\Delta E(\mathbf{h})\exp[-U_{\text{eff}}(\mathbf{h})/k_B T_0] = f(T_0)$, where $f(T_0)$ depends on the initial temperature only. Since the fastest field dependence comes from the exponent, the shape of the stability diagram should correlate with the horizontal cross section of $U_{\text{eff}}(h_x, h_z)$ shown in Fig. 1(b). Note that the cross section of $U_{\text{eff}}(h_x, h_z)$ also determines the stability against slow relaxation given by the condition $\Gamma t < 1$, with t being the characteristic time of the experiment. The stability against avalanches and slow relaxation is illustrated in Fig. 2.

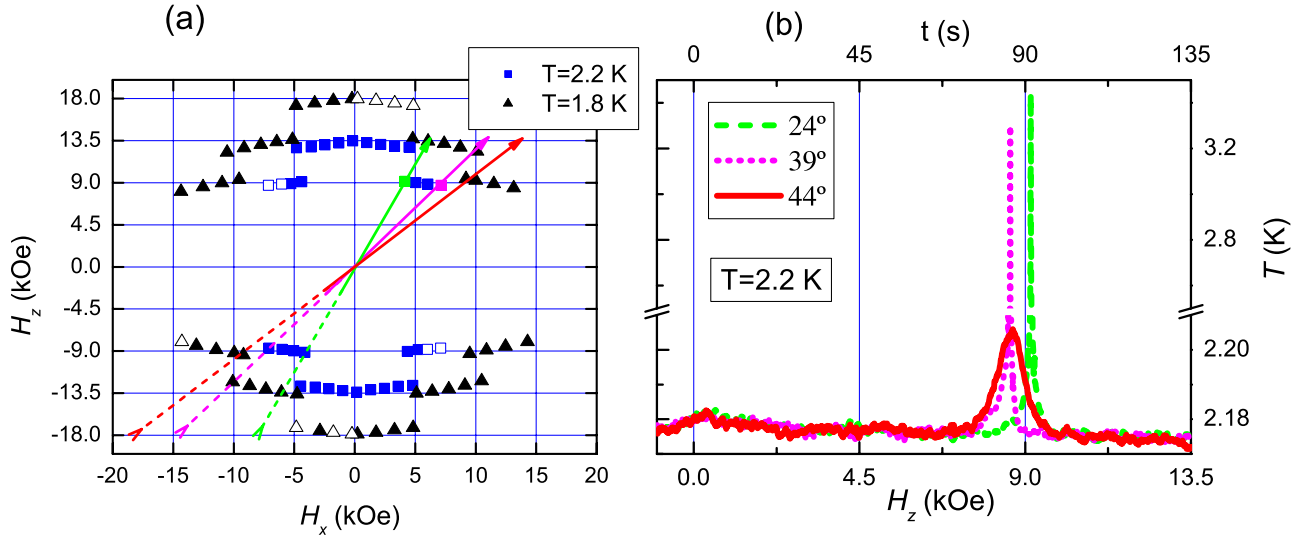


FIG. 3. (Color online) (a) Angle dependence of the metastability area measured through the occurrence of avalanches. Black triangles are for $T_0=1.8$ K while blue squares are for $T_0=2.2$ K. Nonsolid symbols are images of symmetrically measured points. (b) Temperature data for field sweeps at different angles; the three curves correspond to 24° , 39° , and 44° , respectively, at $T=2.2$ K.

For an avalanche to occur for a given field orientation and a constant field-sweep rate, the $h_z(h_x)$ curve obtained from the ignition threshold, $U_{\text{eff}}\Delta E \exp(-U_{\text{eff}}/k_B T) = f(T_0)$, should be crossed before the curve describing stability against slow relaxation, $U_{\text{eff}} = k_B T_0 \ln(t/\tau_0)$. At a given temperature, there is a critical angle, θ_c , below which the avalanche can occur. Above this angle, slow relaxation reduces flammability, bringing it under the avalanche threshold before an avalanche can actually take place. We emphasize here the influence of different measuring conditions. The measuring time does affect directly the threshold $\Gamma t > 1$. In fact, one should generalize this condition to $\int_0^t \Gamma dt > 1$; assuming a linear field-sweep rate, $H = at$, the condition becomes $\int_0^H \Gamma dH > \alpha$. The shape and size of the crystal also affects the parameter l in Eq. (5). We found that the most significant result affected by the measurement setup and/or the crystal shape/size was the crossing point (θ_c) between the slow relaxation and avalanche stability curves.

Experiments were carried out using a commercial magnetometer configured with a 7 T horizontal split-pair magnet. The magnetic properties of the $\text{Mn}_{12}\text{-Ac}$ single crystals were found to be similar to those previously published.^{4,6,14–16} We used a relatively large crystal of $\text{Mn}_{12}\text{-Ac}$ that was about 2 mm long and 0.5 mm wide. Smaller crystals did not show magnetic avalanches on sweeping the magnetic field due to rapid escape of heat through the surface (i.e., the magnetization relaxes slowly with increasing magnetic field before the avalanche condition is achieved). The sample was placed on a plastic stand at the end of a probe, which was inserted into the magnet cryostat; the probe enabled rotation of the sample relative to the applied magnetic field with 0.1° precision. The field was swept back and forth between large negative and positive values ($H = \pm 3$ T), thus ensuring that the sample was saturated with all spins in one well at the beginning of each sweep cycle. The sweep rate was kept constant at 100 Oe/s in all experiments. A very small thermometer ($1 \times 1 \times 0.3$ mm²) was attached as close as possible to the sample

in order to detect not only the temperature rise during an avalanche but also the small changes in the temperature preceding an avalanche. The maximum measured temperatures are not expected to correspond to the flame temperature because of the narrow width and rapid motion of the deflagration front.

The measured stability diagram is shown in Fig. 3(a). In our experiments, avalanches appeared only at resonance fields. The similarity between the experiment [Fig. 3(a)] and theory (Fig. 2) is clear. The decrease in the stability area with increasing temperature is also in accordance with theoretical predictions. Thermal data obtained during field sweeps are shown in Fig. 3(b) for different field orientations for $T_0 = 2.2$ K. Two of the (dashed purple and dotted green) curves show an abrupt increase, whereas the other (straight red line) has a smooth and much smaller perturbation. The observed maxima are due to accelerated relaxation at the second resonance. The two sweeps with abrupt maxima correspond to avalanches and the smooth evolution to a slow relaxation. The magnetic field was applied at $\theta = 24^\circ$ and $\theta = 39^\circ$ with respect to the anisotropy axis for the curves showing avalanches. The $\theta = 44^\circ$ curve exhibits slow relaxation. For this field sweep rate (100 Oe/s) and temperature, avalanches were detected up to a certain critical angle, θ_c , above which only slow relaxations were observed in accordance with Fig. 2 and the above discussion.

Finally, we consider the appropriateness of the underlying quantum mechanical expressions used in evaluating U_{eff} , i.e., Eqs. (1) and (3). Certainly, they ignore interactions which are known to influence tunneling, e.g., high-order transverse zero-field anisotropy terms.¹⁷ We stress that the details of these transverse terms do not qualitatively influence the findings of this study. The shapes of the stability curves are determined primarily by the axial anisotropy parameter D , while the transverse terms mainly affect the depths of the channels which cut into the classical astroid [see Fig. 1(b)]. It is within these channels that one observes quantum relax-

ation, either via slow tunneling or deflagration. Which of these processes occurs depends on the ratio of h_x and h_z , i.e., θ . In other words, for sufficiently strong transverse fields, one expects the slow relaxation to reduce the flammability of the metastable magnetization to a level below which avalanches can no longer occur. Therefore, our findings should apply quite generally.

In summary we have measured the stability of a Mn_{12} -Ac crystal against magnetic avalanches as a function of the angle that the magnetic field makes with the anisotropy axis. Our findings agree with the theory of magnetic deflagration. They demonstrate that experiments on magnetic deflagration provide a powerful tool for comprehensive nondestructive studies of combustion. In such experiments one can easily change the energy barrier and the released heat by varying the magnetic field. The magnetic flammability of the material

can be also varied by changing the initial magnetization. In addition to features commonly seen in combustion, the stability diagram of Mn_{12} -Ac exhibits clear quantum features that distinguish magnetic deflagration from chemical burning. As far as we know, it has not been observed in any other substance. While this Brief Report concentrates on stability only, further studies should elucidate the very interesting physics of what is happening inside the quantum deflagration front.

F.M. thanks the MEyC for a research grant. J.M.H. thanks the MEyC and the Universitat de Barcelona for a Ramón y Cajal research contract. S.H. acknowledges the support of the U.S. National Science Foundation (Grants No. DMR0804408 and No. DMR0414809).

¹I. Glassman, *Combustion* (Academic, New York, 1996).

²A. Hernández-Mínguez, J. M. Hernandez, F. Macià, A. García-Santiago, J. Tejada, and P. V. Santos, *Phys. Rev. Lett.* **95**, 217205 (2005).

³Y. Suzuki *et al.*, *Phys. Rev. Lett.* **95**, 147201 (2005).

⁴E. Chudnovsky and J. Tejada, *Macroscopic Quantum Tunneling of the Magnetic Moment* (Cambridge University Press, Cambridge, 1998).

⁵R. Sessoli, D. Gatteschi, A. Caneschi, and M. A. Novak, *Nature* (London) **365**, 141 (1993).

⁶J. R. Friedman, M. P. Sarachik, J. Tejada, and R. Ziolo, *Phys. Rev. Lett.* **76**, 3830 (1996).

⁷E. del Barco, J. M. Hernandez, M. Sales, J. Tejada, H. Rakoto, J. M. Broto, and E. M. Chudnovsky, *Phys. Rev. B* **60**, 11898 (1999).

⁸F. Fominaya, J. Villain, P. Gandit, J. Chaussy, and A. Caneschi, *Phys. Rev. Lett.* **79**, 1126 (1997).

⁹C. Paulsen and J.-G. Park, in *Quantum Tunneling of Magnetization—QTM'94*, edited by L. Gunther and B. Barbara

(Kluwer, Dordrecht, 1995).

¹⁰S. McHugh, R. Jaafar, M. P. Sarachik, Y. Myasoedov, A. Finkler, H. Shtrikman, E. Zeldov, R. Bagai, and G. Christou, *Phys. Rev. B* **76**, 172410 (2007).

¹¹D. Garanin, arXiv:0805.0391 (unpublished).

¹²D. A. Garanin and E. M. Chudnovsky, *Phys. Rev. B* **56**, 11102 (1997).

¹³D. A. Garanin and E. M. Chudnovsky, *Phys. Rev. B* **76**, 054410 (2007).

¹⁴B. Barbara, L. Thomas, F. Lioni, I. Chiorescu, and A. Sulpice, *J. Magn. Magn. Mater.* **200**, 167 (1999).

¹⁵E. del Barco, A. Kent, S. Hill, J. North, N. Dalal, E. Rumberger, D. Hendrickson, N. Chakov, and G. Christou, *J. Low Temp. Phys.* **140**, 119 (2005).

¹⁶D. Gatteschi and R. Sessoli, *Angew. Chem., Int. Ed.* **42**, 268 (2003).

¹⁷S. Carretta, E. Livioti, N. Magnani, P. Santini, and G. Amoretti, *Phys. Rev. Lett.* **92**, 207205 (2004).